Arm rehabilitation with a robotic exoskeleleton in Virtual Reality

Antonio Frisoli*, Luigi Borelli*, Alberto Montagner*, Simone Marcheschi*, Caterina Procopio*, Fabio Salsedo*, Massimo Bergamasco*, Maria C. Carboncini†, Martina Tolaini†, Bruno Rossi†

***Abstract*— Several studies demonstrate the importance of an early, constant and intensive rehabilitation following cerebral accidents. This kind of therapy is an expensive procedure in terms of human resources and time, and the increase of both life expectance of world population and incidence of stroke is making the administration of such therapies more and more important. The development of new robotic devices for rehabilitation can help to reduce this cost and lead to new effective therapeutic procedures.**

In this paper we present an exoskeleton for the robotic-assisted rehabilitation of the upper limb. This article describes the main issues in the design of an exoskeletal robot with high performance, in terms of backdrivability, low inertia, large workspace isomorphic to the human arm and high payload to weight ratio. The implementation of three different robotic schemes of therapy in virtual reality with this exoskeleton, based on an impedance control architecture, are presented and discussed in detail. Finally the experimental results of a preliminary evaluation of functionality of the system carried out on one patient are presented, and compared with the performance in the execution of the exercise obtained with healthy volunteers. Moreover, other preliminary results from an extended pilot clinical study with the L-Exos are reported and discussed.

I. Introduction

The impairment of upper limb function is one of the most common and challenging sequelae following stroke, that limits the patient's autonomy in daily living and may lead to permanent disability [1]. Although stroke incidence data may differ significantly between different countries, it is to be noted that Italian statistics [2] show that 30% of stroke patients suffer from Activities of Daily Living (ADL) limiting disabilities, arm paralysis or arm paresis being the most common. Partial or total motor functionality recover is therefore without a doubt a fundamental prerequisite leading to major improvements in the quality of life for stroke patients. On this basis, the creation of effective robotic rehabilitation devices which allow significant motor recovery in chronic stroke patients has become an actual and challenging research area.

Well-established traditional stroke rehabilitation techniques rely on thorough and constant exercise [3], [4], which patients are required to carry out within the hospital with the help of therapists, as well as during daily life at home. Early initiation of active movements by means of repetitive training has proved its efficacy in guaranteeing a good level of motor capability recovery [5]. Such techniques allow stroke patients to partly or fully recover motor functionalities of the hemiparetic side limbs during the acute stroke phase, due to the clinical evidence of a period of rapid sensorimotor recovery in the first three months after stroke, after which improvement occurs more gradually for a period of up to two years and perhaps longer [6], [7]. However, permanent disabilities are likely to be present in the chronic phase, after usual therapies. In particular, a satisfying upper extremity motor recovery is much more difficult to obtain with respect to lower extremities [8].

Several studies have attempted to investigate the efficacy of stroke rehabilitation approaches [9], [10]. Intensive and task oriented therapy for the upper limb, consisting of active, highly repetitive movements, is one of the most effective approaches to arm function restoration [11], [12]. The driving motivation to apply robotic technology to stroke rehabilitation is that it may overcome some of the major limitations manual assisted movement training suffers from, i.e. lack of repeatability, lack of objective estimation of rehabilitation progress, and the high dependence on specialized personnel availability. In addition, Virtual Reality can provide a unique medium where therapy can be provided within a functional and highly motivating context and can be readily graded and documented. The cortical reorganization and associated functional motor recovery after Virtual Reality treatments in patient with chronic stroke are documented also by fRMN [13].

Among leg rehabilitation robot devices, Lokomat [14] has become a commercial and widely diffused lower limb robotic rehabilitation device. It is a motorized orthosis able to guide knee and ankle movements while the patient walks on a treadmill. Concerning arm rehabilitation devices, both cartesian and exoskeleton-based devices have been developed in the last 10 years. Some of them will now be briefly described from a design perspective.

MIT Manus [15], [16] and its commercial version InMotion2 [17] are pantograph-based planar manipulators, which have extensively been used to train patients on reaching exercises and have been constantly evaluated by means of clinical data analysis [18]. The machine is 3-DoF, 2 of which being actuated. It has been designed to be backdriveable as much as possible and to have a nearly isotropic inertia. ARM-guide [19], [20] is a device which attaches to the patient's forearm and guides the arm along a linear path having a variable angle with respect to the horizontal position. Constraint forces and range of motion are measured throughout the exercises. The MIME (Mirror Image Movement Enabler) system [21] is a bimanual robotic device which uses an industrial PUMA

* PERCRO, Scuola Superiore Sant'Anna, Pisa, Italy. For communications, please contact a.frisoli@sssup.it.

† Unit of NeuroRehabilitation, Department of Neurosciences, University of Pisa.

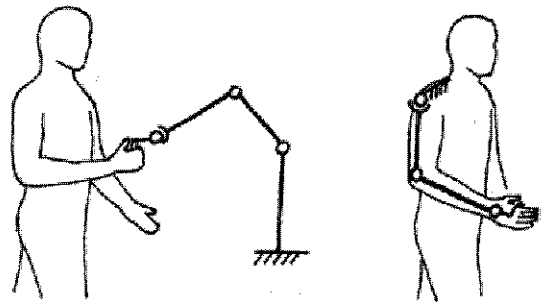

Fig. 1. A comparison between the kinematic schemes of a classical manipulator and an exoskeleton system

Fig. 1

560 robot that applies forces to the paretic limb during 3-dimensional movements. The system is able to replicate the movements of the non-paretic limb.

Exoskeletons are robotic systems designed to work linked with parts (or the whole) of the human body, as shown in Figure 1. In general robots are designed for a defined workspace where they perform specific tasks autonomously [22]. In such a condition, the issue of the physical interaction between robots and humans is considered in terms of safety. The design of exoskeleton systems stems from opposite motivations that intend the robotic structure to be always maintained in contact with the human operators limb. Such a condition is required for several applications that include the use of master robotic arms for teleoperation, active ortheses and rehabilitation [23].

The condition of physical contact between the exoskeleton and the human body is not related to a single point of contact, like it happens for haptic interfaces presenting a stylus at the end-effector grasped by the human operator. The physical link between the exoskeleton and the human body refers to several points of attachment, usually at least one for each limb: in such a condition the exoskeleton robotic structure presents two possible simultaneous functionalities:

1) Following and tracking the body movements in terms of the complete spatial configuration of the limb;
2) Being able to generate forces and exert them to the human body through the points of attachment.

The strict correspondence of the exoskeleton workspace with the human limbs workspace defines constraints for the kinematics and range of joint motions of the exoskeleton robotic structure.

Another design constraint is represented by the simultaneous presence of the limb volume and the robotic structure: due to the physical continuity of the body, the mechanical structure of the exoskeleton cannot occupy the same limbs volume and, consequently, it is usually shaped in order to wrap up the limb itself.

Since the beginning of the research in teleoperation, robotic exoskeletons have been devised as natural solutions for master arms since they allowed the tracking of the human operators arm in a direct and immediate way. Experiments on exoskeletons have been performed also at the JPL during 1970s [24]. Sarcos [25] developed a master arm integrating also grasping capabilities for the hand used for the remote control of a robotic arm, while at PERCRO arm exoskeletons have been developed for interaction with virtual environments since 1994 [23], [26], [27]. Exoskeletons can be suitably employed in robotic assisted rehabilitation [28].

Two exoskeleton-based systems have been developed at Saga University, Japan. The older one [29] is a 1-DoF interface for the human elbow motion, where angular position and impedance of the robot are tuned relying on biological signals used to interpret the human subjects intention. The newer neuro-fuzzy controlled device [30] is a 2-DoF interface used to assist human shoulder joint movement. Another device, the ARMin, has been developed at ETH, Switzerland [31], [32]. This device provides three active DoFs for shoulder and one active DoF for elbow actuation. The patient is required to perform task-oriented repetitive movements having continuous visual, auditory and haptic feedback. Salford Exoskeleton [33], which is based on pneumatic Muscle Actuators (pMA) and provides an excellent power over weight ratio, has also been used in physiotherapy and training

A recent survey [34] on the efficacy of different robot assisted therapies outlines that robotic-aided therapy allows a higher level of improvement of motor control if compared to conventional therapy. Nevertheless, it is to be noted that no consistent influence on functional abilities has yet been found.

In this paper we present the design of the L-Exos system [35], which is a force-feedback exoskeleton for the right arm, and its application for robotic-assisted rehabilitation. Many technical details of the L-Exos system have already been presented in [27]. Some of them will be shortly reviewed within this paper, underlining why such structure is suitable for arm robotic rehabilitation, which improvements have been implemented in order to use the device with stroke patients, which is the structure of the control architecture, and which VR-aided rehabilitation protocols have been implemented. In particular, three different schemes of therapy in virtual reality are presented in terms of control architecture and description of the task. The experimental results of a preliminary evaluation conducted with one patient and with healthy subjects are then reported and discussed. Moreover, other preliminary results from a pilot study which is currently taking place with the L-Exos are reported and discussed.

II. The L-EXOS system

L-EXOS (Light Exoskeleton) [35] is a force-feedback exoskeleton for the human arm. The L-Exos has been designed as a wearable interface, capable of providing a controllable force at the center of user's right-hand palm, oriented along any direction of the space, through a handle that can be grasped by the user, as shown in Figure 2. A button placed on the handle allows to perform basic selection operations in the virtual environment.

Fig. 2. The L-EXOS worn by a user.

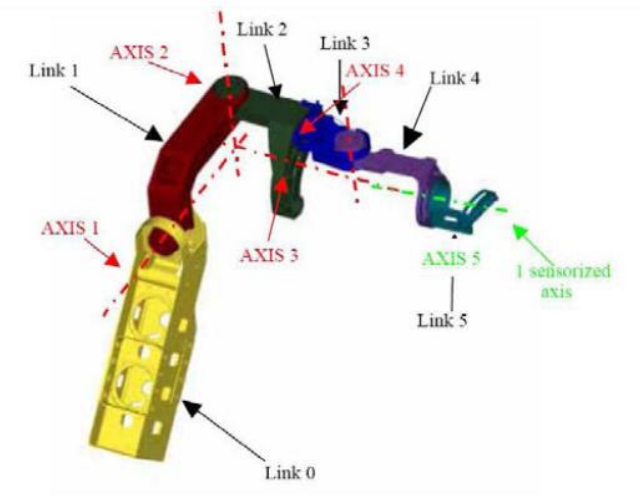

Fig. 3. The general kinematics of the L-Exos

A. *Specifications for rehabilitation*

The main requirements which have been identified for an exoskeleton-based robotic device and for the related VR system in order to be used for neurorehabilitation are here reported:

- Easily wearable and usable structure
- Ability to apply forces to the end-effector in the range of 0-100N
- High correspondance of the robot workspace to an average human arm workspace
- Tridimensional exercises in a Virtual Environment with a scalable mapping from end-effector to virtual displacements
- Compliancy with possible motor compensation strategies employed by chronic stroke patients
- Active and tunable arm weight compensation
- VR development environment for rapid prototyping of exercises
- Overall system safety

B. *Kinematics*

L-exos is characterized by a serial kinematics consisting of five rotational joints, as shown in Figure 3, of which the first four ones are actuated and sensorized, while the last one is only sensorized. Three cartesian hand coordinates (i.e.: positions) are therefore controlled by means of four actuators. The system is redundant in order to comply with motor compensation strategies possibly performed by patients (e.g.: elbow movements). The 5th DoF is passive and allows free wrist pronation and supination movements.

The first three rotational axes are incident and mutually orthogonal (two by two) in order to emulate the kinematics of a spherical joint with the same center of rotation of the human shoulder. The target workspace for the shoulder joint was assumed to be the quadrant of a sphere, as shown in Figure 4. It is to be noted that the exoskeleton shoulder joint has a fixed position in space, whereas the human shoulder joint is not a perfect spherical joint, and its centre may vary with respect to different arm postures. Such aspect is considered not to lead to major problems for the application of the L-Exos to arm rehabilitation, due to the low level of excursion which is foreseen for the shoulder joint while performing rehabilitation exercises. Moreover, the user's shoulder is not physically constrained to the exoskeleton device, thus allowing a greater motion freedom while performing the required tasks.

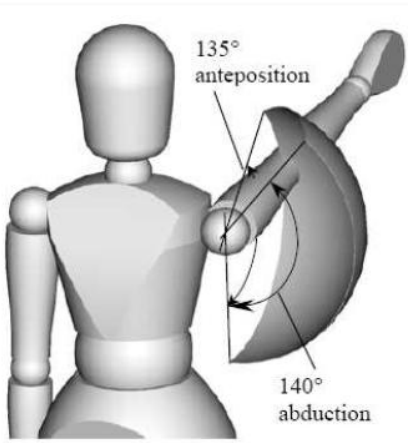

Fig. 4. The reachable workspace of the arm exoskeleton

The axes maximum angular displacements, which are measured from initial to final end-stop positions, are reported in Table I. The described configuration may be thought as isomorphic to the human arm, and the reachable workspace allowed by the structure corresponds to about 70% of the reachable workspace of average healthy subjects.

C. *Mechanical Design*

In order to improve the transparency of use of the device, a set of guidelines have been adopted for the mechanical design:

TABLE I
AXIS MINIMUM AND MAXIMUM ANGULAR POSITIONS

Axis n.	Angular range
1	120°
2	135°
3	140°
4	105°
5	180°

- Remote placement of motors: this allows to drastically reduce the perceived inertia (increase of interface transparency) and the joint torque required for the gravitational compensation, and so the motors size and the transmissions tension;
- Selection of motors with high torque to weight ratio;
- Use of tendon transmissions: even though they have low stiffness, they can easily transmit torques to joints placed far apart from motors with zero backlash, low friction and low weight. Moreover, cable transmissions are more efficient than gear transmissions, thus ensuring a better backdrivability grade for the system;
- Low transmission ratio: this allows to reduce the contribution of the motors to the perceived inertia at the end-effector and so to lower the perceived transmission friction;
- Low or zero backlash implementation of the joints;
- Use of light materials for the construction of the moving parts;
- Guarantee of a safe, comfortable and ergonomic use of device.

All the motors of the exoskeleton have been located on the fixed frame (Link 0). For each actuated DoF, the torque is delivered from the motor to the corresponding joint by means of steel cables and a reduction gear integrated at the joint axis, as shown in Figure 5. Such an arrangement allows to reduce the masses of the moving parts, by reducing the mass of the motors (near 40% of the overall mass of the exoskeleton) and the additional mass of the structural parts, to be reinforced in order to sustain the weight of heavier motors. The inertia perceived by the user at the palm is also consequently reduced. Vernitron 3730V-115 electric actuators have been selected due to their high torque to weight ratio (3.7Nm peak torque vs 650g weight) and torque to volume (thanks to their hollow cylindrical structure) ratio.

In order to ground the motors long transmissions through steel cables were implemented that can guarantee low weight and zero backlash, as shown in Figure 6.

To achieve a higher stiffness of the device at the end effector, specially designed reduction gears with low reduction ratio (between 4 and 6, depending on the joint, guaranteeing an additional mass due to the gear of 345 to 360 grams) have been integrated with each joint, thus allowing to reduce the tendon tensions, their elongation and their diameter. The reduction of the tendon diameter led to a consequent saving of mass and volume of all the mechanical parts of

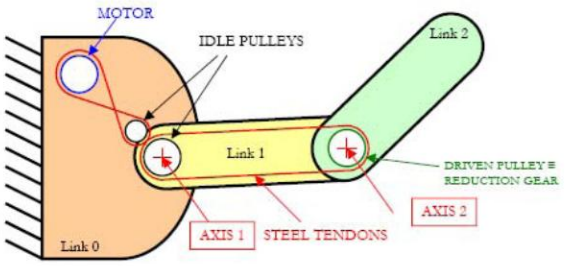

Fig. 5. Scheme of the actuation of the joint 2 of the L-Exos.

the transmission system (pulleys, axles, etc). Thanks to this solution and to the development of expressly conceived speed reducers a mass reduction of about 40% for the structural parts has been achieved, and the transmission system has a lower mass with respect to more traditional motion and force transmission solutions. The structural components (links) have been designed as thin-wall parts, that can house the mechanical parts of the transmission (pulleys, tendons, axles, spacers, etc) within the links, protecting the inner parts from external interference and the user from potential harm deriving by the tensed steel cables.

Hollow sections, presenting a larger moment of inertia than bulk sections with the same area, were used to enhance the stiffness of the thin-wall parts. In order to further improve lightness and stiffness, the structural components were made of carbon fiber. Also aluminum parts were bonded on the carbon fiber structure to realize the connections with other mechanical components.

The carbon fiber parts were manufactured with the vacuum-bag technique, and with dies made of carbon fiber too, due to the low number of prototypes manufactured.

D. Performance of the L-Exos

The L-EXOS can attain very remarkable performance, that can be summarized as follows:

Force	50 N continuous, 100 N peak force;
Backlash	10 mm at the end effector;
Stiffness	Estimated 3 N/mm, measured 2 N/mm (in worst-case condition);
Workspace	approxim. 70% of that of human arm.

The L-Exos has a weight of 11 kg, of which approximately 6 kg distributed on the link 0, i.e. the fixed part, and mostly due to the mass of the 4 motor-groups. This means the L-EXOS achieve a weight/payload ratio close to one (100N vs. 11 Kg).

III. A PRELIMINARY CLINICAL TRIAL

The L-EXOS system is currently installed at the Neurorehabilitation Unit, University of Pisa, where the robotic arm is integrated with a video projection system for the visualization of the virtual environment and is currently being employed in schemes of robotic assisted rehabilitation. The patient is sat down on a seat as shown in Figure 9(d), with his/her right forearm wearing the exoskeleton and

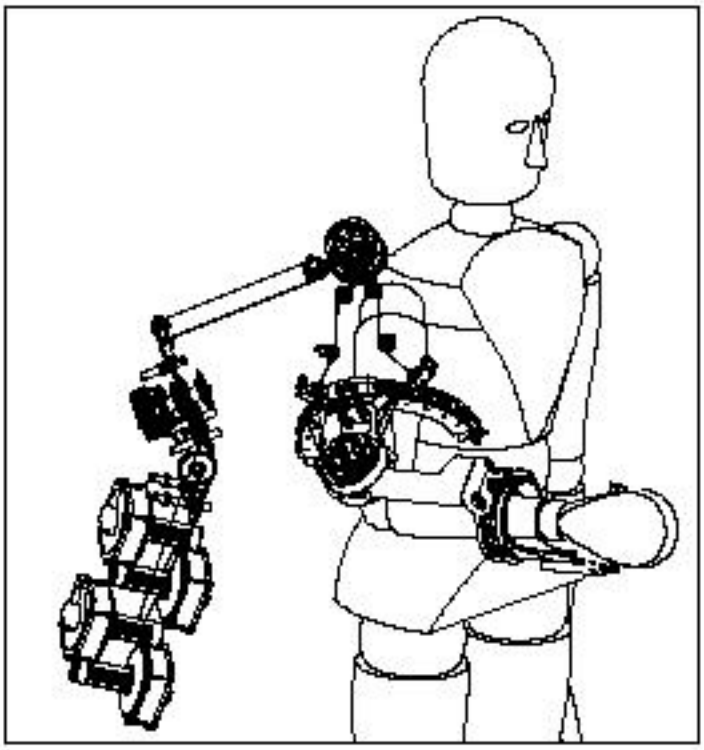

Fig. 6. CAD model of the transmission system

a video projector displaying frontally the virtual scenario. A schematic representation of the actual integrated system layout is shown in Figure 7.

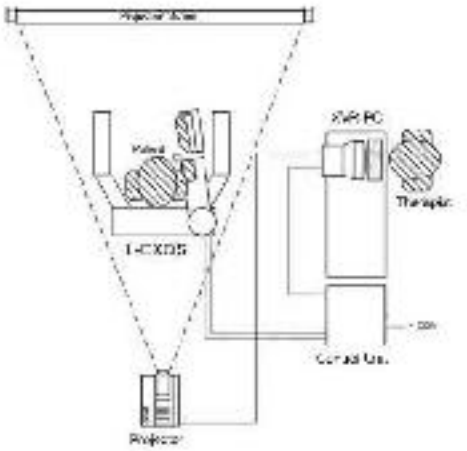

Fig. 7. Actual system layout

All the 3D scenarios have been developed through the XVR development platform for virtual reality applications [36]. A preliminary clinical test has been conducted to evaluate the ergonomics of the system and the functionality as a rehabilitation device on a set of three different applications. The test was intended to demonstrate that the L-Exos can be successfully employed by a patient and to measure the expected performance during therapy.

To assess the functionality of the device, three different tasks and corresponding exercises have been devised and are presented in the following sections:

- A reaching task;
- A free motion task constrained to a circular trajectory;
- A task of object manipulation.

The tasks are thought in order to be executed in succession within one therapy session of the duration of about one hour, to be repeated three times for week.

A. Reaching task

In the first task, the represented scenario is composed of a virtual room, where different fixed targets are displayed to the patient as gray spheres disposed on a horizontal row, as shown in Figure 8. The position of the hand of the patient is shown as a green sphere, that is moved according to the end-effector movements.

The starting position of the task was chosen as a rest position of the arm, with the elbow flexed at 90°, as shown in Figure 9(a). In this position, the exoskeleton provides the support for the weight of the arm, so that the patient can comfortably lean his arm on the exoskeleton.

When one of the fixed targets is activated, a straight trajectory connecting the starting point and the final target is displayed in the simulation. The patient is instructed to actively follow the position of a yellow marker, whose motion is generated along the line connecting the start and end points according to a minimum jerk model [37], approximated by a 5^{th} degree polynomial with a displacement profile as represented in figure 10.

The patient is asked to move the arm to reach the final target with a given velocity, minimizing the position error

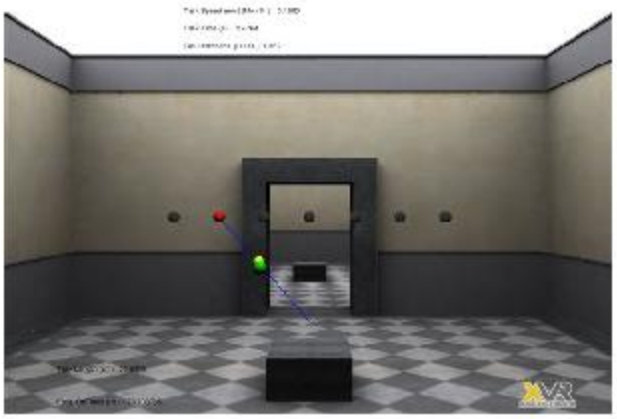

Fig. 8. The virtual scenario visualized in the reaching task

(a) The starting position of the reaching task.

(b) A subject in the middle of the path of the reaching task

(c) A subject at the end-point of the path of the reaching task

(d) The overall system.

Fig. 9. The arm exoskeleton during the execution of the reaching task

between the yellow marker that moves automatically toward the target, and his/her own marker, represented by the green sphere. The yellow marker reaches the target with zero velocity, and comes back on the blue line towards the initial position. The patient is alerted of the start of the exercise by a sound, that is generated automatically by the system. The therapist can set the maximum speed of the task, by choosing among three maximum speeds ($v_1 = 5$ cm/s, $v_2 = 10$ cm/s and $v_3 = 15$ cm/s) and change the position of the fixed targets that should be reached by the patient, both in terms of target height and depth within the virtual room.

The movement towards multiple targets disposed on the same row and backwards is activated in sequence, so that the patient can perform movements in both medial and lateral planes, reaching targets at the same height. There are 7 fixed targets placed symmetrically respect to the sagittal plane of the subject and the fixed targets can be disposed at two different heights relative to the start position of the task ($h_1 = 0.01$ m and $h_2 = 0.12$ m). During each series, the height of the fixed target is not changed, and the following steps are executed in succession for each series:

1) The first movement is executed towards the leftmost fixed target;
2) Once the fixed target is reached the moving marker returns back to its start position, it stops for 2 seconds, and then it starts again towards the next target on the right.
3) The last target of each series is the rightmost one.

In order to leave the patient the possibility to actively conduct the task and being passively guided by the robot only when he/she is unable to complete the reaching task, a suitable impedance control has been developed.

The control of the device is based on two concurrent impedance controls as shown in Figure 11, acting respectively along tangential and orthogonal directions to the trajectory. Each of the two models use a centralized cartesian PD control to calculate the force to exert at the robot end-effector.

With reference to figure 11, $\mathbf{x}_{des}$ is the target position generated by the minimum-jerk model, $\mathbf{e}_n$ and $\mathbf{e}_t$ the tangential and normal position errors, $\mathbf{F}$ the desired wrench applied on the operator's hand and τ is the vector of the joint torques, J is the jacobian of the exoskeleton depending on the joint position vector $\mathbf{q}$, DK represents the direct kinematic algorithm of the device, $G(\mathbf{q})$ are the gravity torques and τ_h are the torques applied by the operator wearing the exoskeleton.

In quasi-static conditions and with gravity, the mapping between the applied wrench and the joint torques can be derived by means of the principle of virtual works and is given by the transpose jacobian of the manipulator:

$$\tau \cong G(\mathbf{q}) + J^T(\mathbf{q})\mathbf{F} + \tau_h \quad (1)$$

The desired force $\mathbf{F}$ is computed according to the error $\mathbf{e} = \mathbf{x}_{des} - \mathbf{x}$ between the desired position $\mathbf{x}_{des}$ and the actual end-effector position $\mathbf{x}$, derived by the DK algorithm from joint measurements $\mathbf{q}$. The error is projected along the two orthogonal directions $\mathbf{e}_n$ and $\mathbf{e}_t$ and the desired force $\mathbf{F}$ is computed as:

$$\mathbf{F} = \mathbf{F}_n + \mathbf{F}_t = (K_{pn} + sK_{dn})\mathbf{e}_n + (K_{pt} + sK_{dt})\mathbf{e}_t \quad (2)$$

The stiffness values K_{pn} and $K_{pt}$of the two models expressed in a cartesian system have been set to respectively

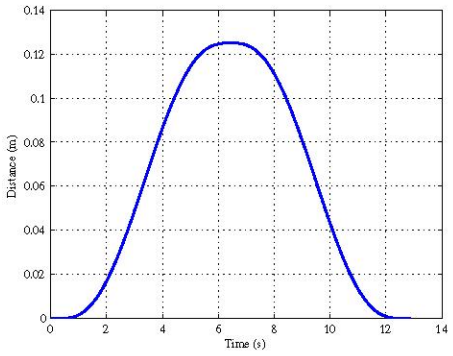

Fig. 10. The motion profile to be followed by the patient in the reaching task

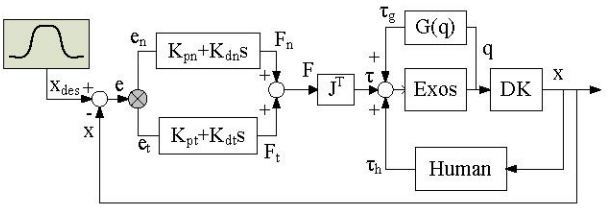

Fig. 11. The impedance control scheme of the device in the reaching task

1200 N/m and 500 N/m for the two directions. A lower stiffness along the trajectory, due to the backdrivability of the system, allows the user to actively perform the task, while the value K_{pn} provides a visual feedback of the error due to uncorrect synergistic muscle activation.

B. Free motion task

In the second exercise the patient is asked to move freely along a circular trajectory, as shown in Figure 12, where it is constrained by an impedance control. The virtual constraint is activated through a button located on the handle. Position, orientation and scale of the circular trajectory can be changed online, thus allowing the patient to move within different effective workspaces. No guiding force is applied to the patient's limb when he/she is moving within the given trajectory, along which the patient is constrained by means of virtual springs.

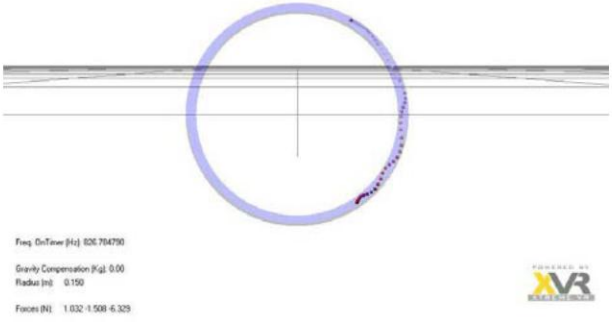

Fig. 12. Example of the free motion constrained to a circular trajectory

Also in this task the therapist can actively compensate the weight of the patient's arm through the device, until the patient is able to autonomously perform the task. This is accomplished by applying torques at the level of the joints, based on a model of the human arm, with masses distributed along the different limbs with a proportion derived from anatomical data. The absolute value of the each limb mass is determined according to the weight of the subject.

C. Task of object manipulation

In this task the patient is asked to move cubes represented in the virtual environment, as shown for instance in figure 13, and to arrange them in a order decided by the therapist, e.g. putting the cubes with the same symbol or with the same color in a row, or putting together the fragments of one image.

For this task the device is controlled with a direct force control, with the interaction force computed by a physics module based on the Ageia PhysX physics engine [38], as shown in Figure 14. By pressing a button on the handle, the patient can decide to select which cube wants to move and release the cube through the same button. Collision with and between the objects are simulated through the physics engine, so that it is actually possibile to perceive all the contact forces during the simulation.

Also in this task the device can apply an active compensation of the weight of the patient arm, leaving to the therapist the possibility to decide the amount of weight reduction.

Fig. 13. An example of task of manipulation of objects

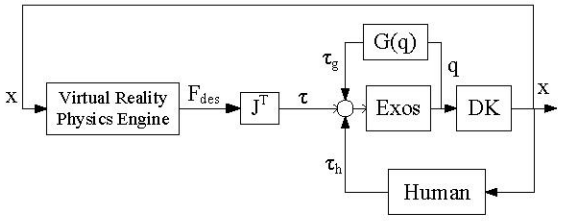

Fig. 14. The control scheme of the device in the manipulation task

IV. Preliminary Results

We have reported briefly in the following the results of a clinical trial performed with a single patient, to assess the overall functionality of the system. The subject involved in the test was a woman aged of 60 that suffered a meningioma in the left hemisphere of the brain that was surgically removed a year before the moment of the test. The disease and the consequent surgical treatment left the subject a reduced mobility of the right upper limb with reduced range of motion of arm articulations (in particular of the distal part of the limb) and reduced speed capabilities. The subject was not previously used to robotic rehabilitation and tried all the three exercises for about one hour.

For the first task of target reaching, the subject executed 6 different series with different heights and velocities. Figure 15 shows the cartesian position components (solid lines) compared to the desired components (dashed lines) of movement for one reaching task ($h_2 = 0.12$ m) performed by the patient at the lowest speed. The task was performed in the frontal plane with the z axis directed opposed to the gravity direction and the y axis along the frontal direction, so that the x coordinate was always kept to zero. The gap between the robot desired position and the patient's hand position is proportional to the force supplied by the robot for completing the task execution. The patient followed quite correctly the trajectory for lower speeds, but the gap increased where the task was executed at higher speeds, as shown in Figure 16(a), where a higher delay appears. This indicates that the patient, being unable to actively accomplish the requested task, lets the device to drag her hand.

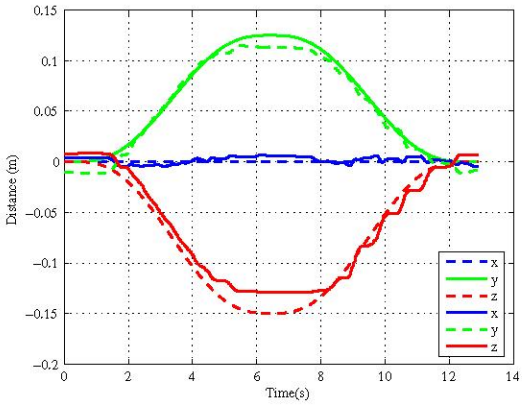

Fig. 15. Patient reaching task at lowest speed $v_1 = 5$ cm/s

It is interesting to compare the performance of an healthy subject with the one of the patient, as shown in Figure 16. In figure 16(b) it is shown the task executed at the same velocity by an healthy subject. The healthy subject is able to actively follow the task and no significant delay is present between the target and the hand position.

This can be explicitly analysed by observing the behavior of the cumulative position error over time, both for the patient and for an healthy volunteer. We can see in figure 17, for two reaching tasks executed in different planes, how

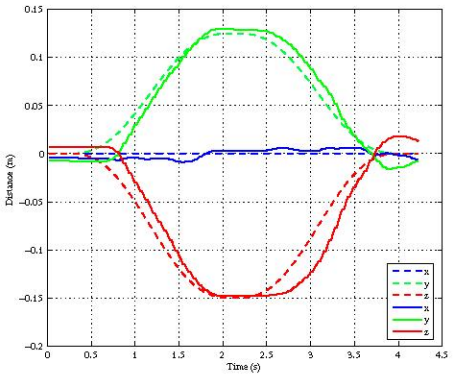

(a) Patient performance.

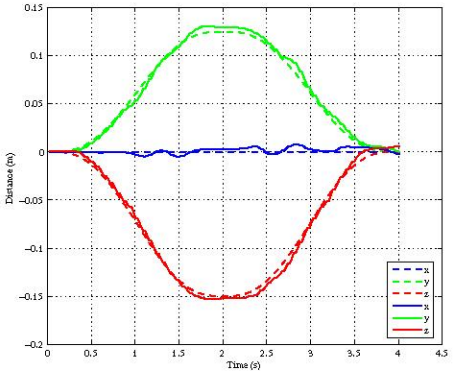

(b) Healthy subject performance.

Fig. 16. Patient vs. healthy subject in the reaching task at the maximum speed $v_3 = 15$ cm/s

the healthy volunteer presents a constant error rate, with the cumulative error increasing linearly over time. On the contrary, the patient presents an error rate composed of three segments with different slope. The first and third segment with higher slope represent the reaching in the forward and backward direction, where a slope higher than the healthy subject indicates a higher average error. The error decreases only in the second segment, that represents the inversion point, where the direction of motion is reversed and the velocity is very low.

For sake of brevity, we do not report here numerical data relative to the execution of the other two exercises. In the free motion task, the patient was not able to execute the exercise until an appropriate level of weight compensation was provided to the arm. After the activation of the weight compensation, the patient was able to correctly execute the task.

In the object manipulation task, it basically emerged how the patient adopted a compensation strategy of movement supplying with the shoulder girdle the full adduction-abduction of the forearm. This indicated how a therapy scheme should consider the adoption of a control with selective compliance of the joints, that can penalize the movement of specific articulations. Due to the antropomorphic kinematics of the exoskeleton, the implementation of such a robotic assisted scheme can be implemented and

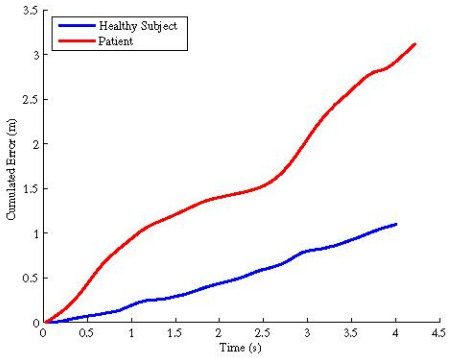

(a) Task in the lateral plane.

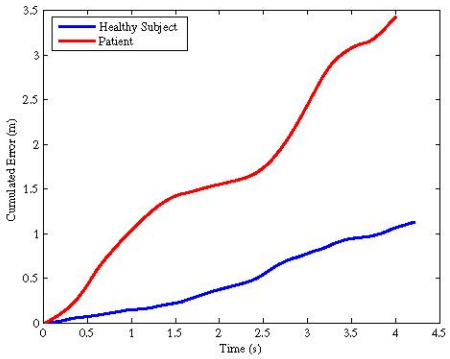

(b) Task in the frontal plane.

Fig. 17. Cumulative position error during task execution $v_3 = 15$ cm/s

represents one of the future aspects to be investigated.

V. Extended clinical trial

At time of writing an evaluation protocol is on-going on a larger sample of patients. In particular, six patients have been selected to undergo a 6-week robotic-assisted therapy, in order to quantitatively evaluate the efficacy of the developed system as a rehabilitation device. A typical therapy session for this clinical trial has a duration of about 60 minutes (50 minutes for the VR exercises + 10 minutes for L-Exos wearing, pauses between exercises, etc), whereas a therapy frequency of 3 sessions per week is used. Inclusion and exclusion criteria for the patient selection will now be reported, as well as preliminar qualitative and quantitative results obtained from the first three patients.

A. Inclusion and exclusion criteria

The inclusion criteria which have been adopted to select the participants are the following:

- Right hemiparetic subjects
- Time from stroke greater than 12 months
- No robotic treatment received before.
- Subjects functionally stables: unchanged motor functions in the last month, despite constant traditional therapy.
- Residual volountary motor control of the right arm with middle-low motor functions.
- Ability to sit for long periods (at least 60 minutes).
- Ability to understand simple commands.

The exclusion criteria which have been adopted to select the participants are the following:

- Bilateral Motor deficit.
- Severe sensorial deficit in the upper right limb.
- Major cognitive deficit (aphasia) that can compromise the understanding of required task.
- Neuromuscular disorders.
- Occipital, cerebellar or brainstem lesions.
- Serious spasticity.
- Apraxia.
- Hemispatial neglect.
- Shoulder subluxation or pain in the upper limb.

B. Clinical situation for admitted patients

Further analysis have been conducted prior to patient admittance to the protocol by means of a motion tracking system and EMG signals. In particular, the relationship between the activation of biceps and triceps muscles with respect to the value of the elbow angle for standard reaching movements (forward and backwards) has been investigated. Some typical plots resulting from this analysis are reported in Figure 18, where angular displacement and rectified EMG data are reported. The three patients present noteworthy differences in muscle activation and maximum elbow angular displacement, which will now be briefly examined.

Patient 1 presents a high level of muscular activation, both for the biceps and the triceps muscles, without any apparent relationship to the phase of the reaching task he is performing. Moreover, the elbow angle spans from a minimum of 75° to a maximum of 110°. The plateau of the elbow angle which is reached while performing the task underlines a limited motion control capability. Further clinical investigations on this patient indicate a severe proprioceptive deficit of Patient 1, who is not able to locate his hand in space without visual feedback of the hand itself.

Patient 2 presents a correct activation pattern while performing the reaching task. The triceps muscle is contracted during the reaching phase, whereas it is released in the backward phase. A complimentary behaviour is shown for the biceps muscle. The elbow angle has a wide span from a minimum of 95° to a maximum of 140°, with a smooth profile indicating a good level of motor coordination.

Patient 3 presents an irregular muscle activation and elbow angle profile while performing the reaching task. Moreover, the elbow angle spans from a minimum of 85° to a maximum of 105°, thus underlining a severe limitation on elbow movements. Further clinical evidence clearly confirm these observations, indicating the presence of shoulder and back compensation strategies during reaching movements.

C. Qualitative results

Qualitative results and patient feedback have been very important in this pilot study in order to guide future developments of the L-Exos for rehabilitation, and they will be now presented. The three patients have been enthusiastic with respect to robotic therapy from the very first trial session

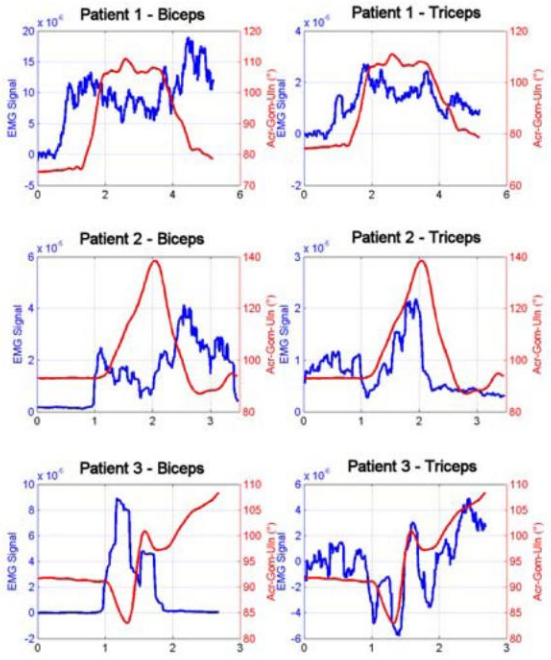

Fig. 18. Motion analysis for the selected patients

with the system, and they have soon gained confidence both with the robotic device and with the personnel (engineers and therapists) involved in the pilot study. The concentration level obtained while performing the proposed exercises has always been very high, thus improving the quality of the therapy. All patients report an increased arm motility after the robotic therapy.

Although quantitative results for the reaching task do confirm such increased motility for Patient 2 and Patient 3, no significant improvement has been demonstrated for Patient 1 after Week 6. Nevertheless, Patient 1 reports much less pain and discomfort when at home, in particular when he is required to sit at a table (e.g.: having lunch) keeping his arm on the table. Moreover, Patient 1 initially reported a high level of discomfort while reaching many of the targets in the reaching task, which has now disappeared. On the other hand, macroscopic benefits have been encountered for Patient 3, who is now able to perform the exercises keeping the back in a correct position. Moreover, by the end of Week 4 an increment of 20% of both speed level and ball horizontal span was possible for this patient.

The three patients are now more comfortable when performing the circle drawing task. In particular, Patient 3, who was initially hardly able to move the exoskeleton without external aid, is now able to perform the required movement at high speed. The same patient is now able to draw much smoother trajectories even without the activation of the impedance controller on the L-Exos, as shown in the comparison of Figure 19. It has to be said that the actual definition of the constrained motion task can sometimes be rather discouraging for the patients who, after following the correct trajectory thanks to the robotic constraint, become skeptical about their improvements after seeing the much more irregular trajectory they can draw without the machine aid.

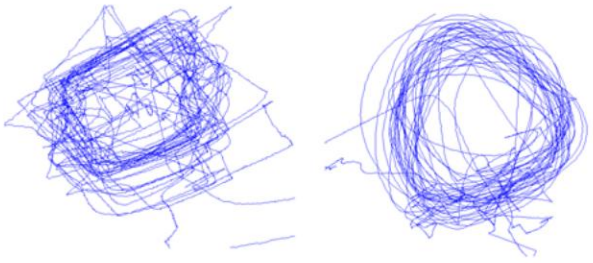

Fig. 19. Free circle drawing - Patient 3 (left: Week 1, right: Week 6)

The object manipulation task has been found interesting for the three patients, who have now become completely familiar with it, and do not require any hint on the best successive move. Moreover, patients initially required a great amount of external help while performing fine movements (e.g.: inserting a cube in a narrow space between two other cubes), which is now much less necessary. It has been found that the proposed image to be reconstructed strongly affects the patient's capability of performing the task.

From a quantitative point of view, joint positions, end-effector positions and forces applied to the end-effector have been recorded throughout the three tasks at a sampling frequency of 100Hz. Preliminary results of this pilot studies will be briefly presented in the following paragraphs for the first two exercises. As a matter of fact, the aim of the third exercise was merely to increase the arm mobility, without any quantitative parameter being monitored.

D. Quantitative results - Reaching

The normalized cumulative error has been chosen as being the most significant metric for a pilot study reaching task data analysis. The normalization parameter has been chosen as the total task time.

No significant data have been obtained for Patient 1, whereas Figure 20 shows the results for the reaching task for Patient 2, who reported the most significant improvement after the therapy. The plots report the cumulative error for each movement performed in the reaching exercise with respect to the task completion percentage. Data were recorded during a session in Week 1 and a session in Week 6. Data have been fit with a 5th order polynomial, the values of which have reduced by 50% after the robotic therapy. Moreover, the variance in the performance between different tasks of a same rehabilitation session has dramatically reduced from initial to final rehabilitation sessions, thus indicating a much more regular and repetitive level of motor coordination. Figure 21 reports the results for the reaching task performed by Patient 3 during Week 1 and Week 6. A mean reduction of the mean cumulative error of about 35% is clearly visible throughout the task, and a reduction in the error variance is clearly visible as well. However, the most significant improvement indicator for Patient 3 is the shape of the cumulative error

curves. In particular, a trilinear-like curve (Week 1) with the typical low-slope, high-slope, low-slope trend indicates that the patient is not able to completely reach the desired end-point, thus making the cumulative error significantly increase in the middle phase of the reaching task. On the other hand, a straight line (Week 6) indicates a constant level of average error, which is independent of the task completion percentage. The Patient has therefore become able to perform the correct motion for the required task.

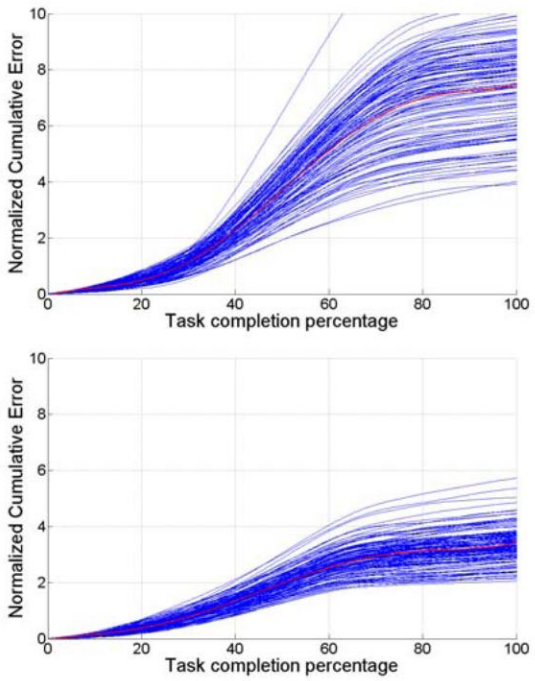

Fig. 20. Reaching results for Patient 2 (up: Week 1, down: Week 6)

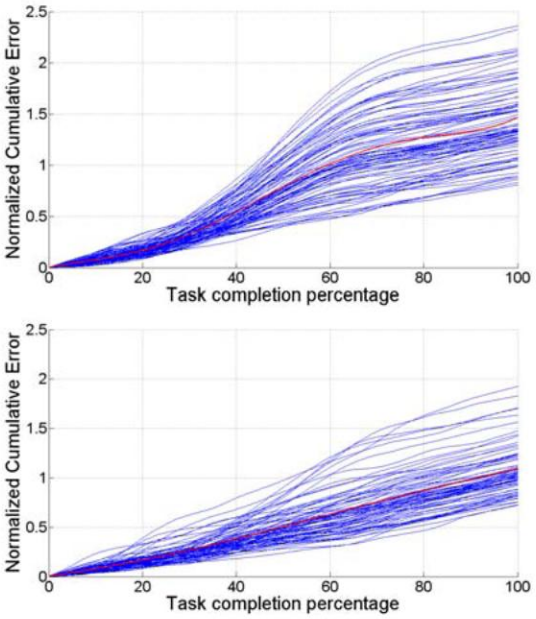

Fig. 21. Reaching results for Patient 3 (up: Week 1, down: Week 6)

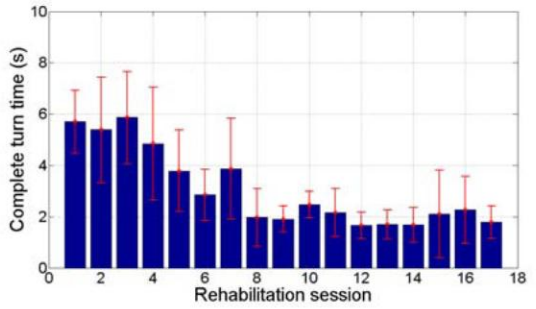

Fig. 22. Constrained motion results for Patient 3

E. Quantitative results - Constrained motion

The parameter which has been used to quantitatively evaluate patients' improvements for the constrained motion task is the total time required to complete a full circular path. 3D position data have been projected onto a best fitting plane (in the sense of least squares), and the best fit circle has been computed for the projected points. The time to accomplish a complete turn has then been evaluated for this latter trajectory. No quantitative data have been computed concerning the curvature along the trajectory, which is still relatively irregular for the three patients. In particular, due to the fact that the implemented stiffness which realizes the motion constraint has deliberately been set to a middle-low value, significant fluctuations around the ideal trajectory are reported for the patients.

Figure 22 shows the results for the constrained motion task for Patient 3, who is the the only patient reporting a statistically significant improvement after the robotic therapy. His turning time was of $5.7s \pm 1.2s$ in session 1, and of $1.7s \pm 0.6s$ in session 13, thus reporting a 70% decrease in the required time to complete the task.

VI. Conclusions and Future Works

In this paper a new exoskeletal device for the rehabilitation of the arm has been presented. The peculiar characteristics of the exoskeleton as its low weight and the high payload make it suitable to be used as an effective aid in automated rehabilitation. The preliminary test carried out with a patient shows that the robot neither hinders the patient movement nor causes uncorrect postures on movements. Furthermore the ability to actively compensate the weight of patient arm turned out to be a powerful tool that allows the patient to execute task that it could not successful accomplish otherwise. It is moreover worthwhile to note that after one hour of exercise the patient reported not to suffer any pain, but to be just a little tired. The patient moreover expressed her enthusiasm towards the system and was very keen to repeat again the robotic-assisted exercises in future sessions. This lead to the start of a longitudinal pilot study, which is currently on-going on a larger sample of patients with stroke impairment, in order to assess the efficacy of robotic assisted therapy. The results obtained so far are encouraging

and strongly suggest to further improve the actual system, both from a software and from a hardware level, in order to widen its range of application. Future work will focus also on the development of single joint impedance controls for the selective penalization of movement of a single articulation.

VII. Acknowledgements

A special thanks goes to Fabrizio Rocchi for its contribution to the preparation of the technical data. This research was partially financed under a research grant by the Fondazione Monte Paschi Siena and by the IP SKILLS research project, funded by the European Commission.

References

[1] H. Nakayama, HS Jorgensen, HO Raaschou, and TS Olsen. Recovery of upper extremity function in stroke patients: the Copenhagen Stroke Study. *Arch Phys Med Rehabil*, 75(4):394–8, 1994.

[2] D. Inzitari. The Italian Guidelines for stroke prevention. The Stroke Prevention and Educational Awareness Diffusion (SPREAD) Collaboration. *Neurol Sci*, 21(1):5–12, 2000.

[3] L. Diller. Post-stroke rehabilitation practice guidelines. *International handbook of neuropsychological rehabilitation. Critical issues in neurorehabilitation. New York: Plenum*, pages 167–82, 2000.

[4] J.H. van der Lee, R.C. Wagenaar, G.J. Lankhorst, T.W. Vogelaar, W.L. Deville, and L.M. Bouter. Forced Use of the Upper Extremity in Chronic Stroke Patients Results From a Single-Blind Randomized Clinical Trial, 1999.

[5] C. Butefisch, H. Hummelsheim, P. Denzler, and KH Mauritz. Repetitive training of isolated movements improves the outcome of motor rehabilitation of the centrally paretic hand. *J Neurol Sci*, 130(1):59–68, 1995.

[6] S. Katz, AB Ford, AB Chinn, et al. Prognosis after stroke: long term outcome of 159 patients. *Medicine*, 45:236–46, 1966.

[7] CE Skilbeck, DT Wade, RL Hewer, and VA Wood. Recovery after stroke. *J Neurol Neurosurg Psychiatry*, 46(1):5–8, 1983.

[8] TS Olsen. Arm and leg paresis as outcome predictors in stroke rehabilitation. *Stroke*, 21(2):247–251, 1990.

[9] E. Ernst. A review of stroke rehabilitation and physiotherapy. *Stroke*, 21(7):1081–1085, 1990.

[10] S.J. Page, P. Levine, S. Sisto, Q. Bond, and M.V. Johnston. Stroke patients' and therapists' opinions of constraint-induced movement therapy. *Clinical Rehabilitation*, 16(1):55, 2002.

[11] S. Barreca, S.L. Wolf, S. Fasoli, and R. Bohannon. Treatment Interventions for the Paretic Upper Limb of Stroke Survivors: A Critical Review. *Neurorehabilitation and Neural Repair*, 17(4):220–226, 2003.

[12] H.M. Feys, W.J. De Weerdt, B.E. Selz, G.A. Cox Steck, R. Spichiger, L.E. Vereeck, K.D. Putman, and G.A. Van Hoydonck. Effect of a Therapeutic Intervention for the Hemiplegic Upper Limb in the Acute Phase After Stroke A Single-Blind, Randomized, Controlled Multicenter Trial, 1998.

[13] SH Jang, S. You, YH Kwon, M. Hallett, MY Lee, and SH Ahn. Reorganization Associated Lower Extremity Motor Recovery As Evidenced by Functional MRI and Diffusion Tensor Tractography in a Stroke Patient. *Restor Neurol & Neurosci*, 23:325–329, 2005.

[14] S. Jezernik, G. Colombo, T. Keller, H. Frueh, and M. Morari. Robotic Orthosis Lokomat: A Rehabilitation and Research Tool. *Neuromodulation*, 6(2):108–115, 2003.

[15] HI Krebs, N. Hogan, ML Aisen, and BT Volpe. Robot-aided neurorehabilitation. *Rehabilitation Engineering, IEEE Transactions on [see also IEEE Trans. on Neural Systems and Rehabilitation]*, 6(1):75–87, 1998.

[16] BT Volpe, HI Krebs, N. Hogan, L. Edelstein, C. Diels, and M. Aisen. A novel approach to stroke rehabilitationRobot-aided sensorimotor stimulation. *Neurology*, 54(10):1938–1944, 2000.

[17] J. Stein, HI Krebs, WR Frontera, SE Fasoli, R. Hughes, and N. Hogan. Comparison of two techniques of robot-aided upper limb exercise training after stroke. *Am J Phys Med Rehabil*, 83(9):720–8, 2004.

[18] SE Fasoli, HI Krebs, J. Stein, WR Frontera, and N. Hogan. Effects of robotic therapy on motor impairment and recovery in chronic stroke. *Arch Phys Med Rehabil*, 84(4):477–82, 2003.

[19] D.J. Reinkensmeyer, J.P.A. Dewald, and W.Z. Rymer. Guidance-Based Quantification of Arm Impairment Following Brain Injury: A Pilot Study. *Rehabilitation Engineering, IEEE Transactions on*, 7(1):1, 1999.

[20] DJ Reinkensmeyer, LE Kahn, M. Averbuch, A. McKenna-Cole, BD Schmit, and WZ Rymer. Understanding and treating arm movement impairment after chronic brain injury: progress with the ARM guide. *J Rehabil Res Dev*, 37(6):653–62, 2000.

[21] PS Lum, CG Burgar, PC Shor, M. Majmundar, and M. Van der Loos. Robot-assisted movement training compared with conventional therapy techniques for the rehabilitation of upper-limb motor function after stroke. *Arch Phys Med Rehabil*, 83(7):952–9, 2002.

[22] CA Avizzano and M. Bergamasco. Technological Aids for the treatment of tremor. *Sixth International Conference on Rehabilitation Robotics (ICORR)*, 1999.

[23] M. Bergamasco. Force replication to the human operator: the development of arm and hand exoskeletons as haptic interfaces. *Proceedings of 7th International Symposium on Robotics Research*, 1997.

[24] BM Jau. Anthropomorhic Exoskeleton dual arm/hand telerobot controller. *Intelligent Robots, 1988., IEEE International Workshop on*, pages 715–718, 1988.

[25] A. Nahvi, DD Nelson, JM Hollerbach, and DE Johnson. Haptic manipulation of virtual mechanisms from mechanical CADdesigns. *Robotics and Automation, 1998. Proceedings. 1998 IEEE International Conference on*, 1, 1998.

[26] M. Bergamasco, B. Allotta, L. Bosio, L. Ferretti, G. Parrini, G.M. Prisco, F. Salsedo, and G. Sartini. An arm exoskeleton system for teleopera-tion and virtual environments applications. In *IEEE Int.Conf.On Robotics and Automation*, pages 1449–1454, 1994.

[27] A. Frisoli, F. Rocchi, S. Marcheschi, A. Dettori, F. Salsedo, and M. Bergamasco. A new force-feedback arm exoskeleton for haptic interaction in virtual environments. *Haptic Interfaces for Virtual Environment and Teleoperator Systems, 2005. WHC 2005. First Joint Eurohaptics Conference and Symposium on*, pages 195–201, 2005.

[28] T. Nef and R. Riener. ARMin-Design of a Novel Arm Rehabilitation Robot. *Rehabilitation Robotics, 2005. ICORR 2005. 9th International Conference on*, pages 57–60, 1928.

[29] K. Kiguchi, S. Kariya, K. Watanabe, K. Izumi, and T. Fukuda. An Exoskeletal Robot for Human Elbow Motion SupportSensor Fusion, Adaptation, and Control. *Systema, man and Cybernetics - Part B: Cybernetics, IEEE Transactions on*, 31(3):353, 2001.

[30] K. Kiguchi, K. Iwami, M. Yasuda, K. Watanabe, and T. Fukuda. An exoskeletal robot for human shoulder joint motion assist. *Mechatronics, IEEE/ASME Transactions on*, 8(1):125–135, 2003.

[31] R. Riener, T. Nef, and G. Colombo. Robot-aided neurorehabilitation of the upper extremities. *Medical and Biological Engineering and Computing*, 43(1):2–10, 2005.

[32] T. Nef and R. Riener. ARMin-Design of a Novel Arm Rehabilitation Robot. *Rehabilitation Robotics, 2005. ICORR 2005. 9th International Conference on*, pages 57–60, 2005.

[33] NG Tsagarakis and D.G. Caldwell. Development and Control of a 'Soft-Actuated' Exoskeleton for Use in Physiotherapy and Training. *Autonomous Robots*, 15(1):21–33, 2003.

[34] GB Prange, MJ Jannink, CG Groothuis-Oudshoorn, HJ Hermens, and MJ Ijzerman. Systematic review of the effect of robot-aided therapy on recovery of the hemiparetic arm after stroke. *J Rehabil Res Dev*, 43(2):171–84, 2006.

[35] F. Salsedo, A. Dettori, A. Frisoli, F. Rocchi, M. Bergamasco, and M. Franceschini. Exoskeleton interface apparatus.

[36] E. Ruffaldi, A. Frisoli, M. Bergamasco, C. Gottlieb, and F. Tecchia. A haptic toolkit for the development of immersive and web-enabled games. *Proceedings of the ACM symposium on Virtual reality software and technology*, pages 320–323, 2006.

[37] DJ Reinkensmeyer, LE Kahn, M. Averbuch, A. McKenna-Cole, BD Schmit, and WZ Rymer. Understanding and treating arm movement impairment after chronic brain injury: progress with the ARM guide. *J Rehabil Res Dev*, 37(6):653–62, 2000.

[38] http://www.ageia.com/.